The Cryosphere Discuss., 4, 1151–1194, 2010
www.the-cryosphere-discuss.net/4/1151/2010/
doi:10.5194/tcd-4-1151-2010

The Cryosphere Discussions

Comparison of direct and geodetic mass balances on a multi-annual time scale

A. Fischer

Institute of Meteorology and Geophysics, University of Innsbruck, Innsbruck, Austria

Received: 28 June 2010 – Accepted: 5 July 2010 – Published: 23 July 2010

Correspondence to: A. Fischer (andrea.fischer@uibk.ac.at)

Published by Copernicus Publications on behalf of the European Geosciences Union.

Abstract

Glacier mass balance is measured with the direct or the geodetic method. In this study, the geodetic mass balances of six Austrian glaciers in 19 periods between 1953 and 2006 are compared to the direct mass balances in the same periods. The mean annual geodetic mass balance for all periods is −0.5 m w.e./year. The mean difference between the geodetic and the direct data is −0.7 m w.e., the minimum −7.3 m w.e. and the maximum 5.6 m w.e. The accuracy of geodetic mass balance resulting from the accuracy of the DEMs ranges from 2 m w.e. for photogrammetric data to 0.002 m w.e. for LIDAR data. Basal melt, seasonal snow cover and density changes of the surface layer contribute up to 0.7 m w.e. for the period of 10 years to the difference to the direct method. The characteristics of published data of Griesgletscher, Gulkana Glacier, Lemon Creek glacier, South Cascade, Storbreen, Storglaciären, and Zongo Glacier is similar to these Austrian glaciers. For 26 analyzed periods with an average length of 18 years the mean difference between the geodetic and the direct data is −0.4 m w.e., the minimum −7.2 m w.e. and the maximum 3.6 m w.e. Longer periods between the acquisition of the DEMs do not necessarily result in a higher accuracy of the geodetic mass balance. Specific glaciers show specific trends of the difference between the direct and the geodetic data according to their type and state. In conclusion, geodetic and direct mass balance data are complementary, but differ systematically.

1 Introduction

Glacier mass balance is a sensitive indicator of climate change. Changes in glacier mass result from ablation and accumulation and is directly related to prevailing atmospheric conditions. Since the glacier mass balance also governs the glacier runoff, it is a valuable parameter for of glaciological modeling with various climatological and hydrological applications. Over the last few years, a major effort was undertaken to

TCD

4, 1151–1194, 2010

Direct and geodetic mass balances on a multi-annual time scale

A. Fischer

estimate the global mass balance of the mountain glaciers and their contribution to sea level rise (Lemke et al., 2007; Kaser et al., 2006).

The mass balance could be determined applying one out of three different methods summarized by Hoinkes (1970):

- the direct or glaciological method
- the geodetic method
- the hydrological-meteorological method

Today, the first two methods are the most commonly used. The direct method requires extensive field work involving field measurements of ablation stakes and snow pits to measure annual ablation and accumulation. The geodetic method uses two or more sets of topographic data, acquired over multi-annual time scales, to calculate volume differences. The direct method allows real-time calculation of glacier mass balances for relatively small glaciers with high temporal and spatial resolution; the geodetic method can be used with remote sensing data. As a result, the geodetic method is often used on large and remote glaciers and ice sheets where extensive filed work would be impractical or too costly, albeit with the disadvantage of lower temporal and spatial resolution. A worldwide dataset analyzed with the geodetic method would not show the representation bias toward small and accessible glaciers naturally present in data derived from direct method observations. Calving glaciers could also be included. The rapid progress in remote sensing techniques and glacier inventories can be expected to provide large data sets suitable for geodetic analysis, and historical topographic records enable to calculation of past glacier mass balances with the geodetic method. The geodetic method of glacier mass balance calculation is an increasingly valuable tool, especially for global glacier mass balances, which are themselves highly relevant to estimates of glacier melt contribution to sea level rise.

To reach a general estimate of the past and current reactions of the cryosphere to climate change, a combination of the different methods is necessary. The higher

TCD
4, 1151–1194, 2010

resolution of the direct method can lead to greater accuracy of measurement and understanding of glacier melt dynamics, while the ease of taking the measurements necessary for the geodetic method enables truly global studies. In order to use the two methods in concert, it must first be ensured that they produce comparable results.

The direct and geodetic mass balance measurements both involve specific assumptions and uncertainties: the calculation of the geodetic mass balance requires assumptions about or measurements of the density of the upper layer of the glacier, while the extrapolation of point measurements to the total glacier area involves assumptions about the spatial distribution of mass balance. To quantify these uncertainties, a number of studies compared the results of the direct mass balance to data derived from the geodetic method. Detailed investigations on Hintereisferner from 1953 to 1964 (Lang and Patzelt, 1971) and later, from 1953 to 1991 (Kuhn et al., 1999), showed good agreement between the geodetic and direct methods. Studies on Gulkana glacier (Cox and March, 2004) and Storglacieren (Zemp et al., 2010) also suggested that the two methods corresponded well. In contrast, Geist and Stötter (2007) showed larger differences between geodetic and direct data collected on Hintereisferner from 2001 to 2005. On the South Cascade glacier, Krimmel (1999) found evidence of a systematic deviation between the two methods.

Several authors have combined direct and geodetic data to produce an optimal mass balance for specific glaciers. This process might reduce random error if the geodetic and direct data do not differ systematically. Huss et al. (2009) combined direct and geodetic data into homogenized mass balance time series of Griesgletscher and Silvrettgletscher in Switzerland. Thibert and Vincent (2009) calculated a combined mass balance for the Glacier de Sarennes.

Today, mass balances of only a small percentage of the world's glaciers are known. Cogley (2009) analysed 344 direct and 327 geodetic mass balance measurements. In total, 1052 years of mass balance data of 59 glaciers have been analyzed by the two methods. About as many glaciers have been observed by the direct as by the geodetic method, but the geodetic data spans four times the number of balance years

TCD
4, 1151–1194, 2010

covered by the direct method. Cogley's statistical analysis showed no evidence of a systematic deviation between geodetic and direct data, but the deviations between the two methods are enormous, reaching more than 1 m w.e. for observed values of +0.5 m w.e. to −2.5 m w.e.

The results cited above suggest one question crucial to future glacier mass balance research: Do data collected and analyzed by the direct method and the geodetic method differ systematically? If so, global studies conducted primarily with the geodetic method could have their accuracy greatly improved by careful comparison to specific direct method calculations. If not, it becomes important to understand why not, and whether the difference between the two methods depends on variables such as the time scale of the study or the sign or magnitude of the mass balance.

The purpose of this study is to answer these questions by investigating direct and geodetic data of six Austrian alpine glaciers in detail over various multi-annual time scales. To investigate the relevance of the results to other regions, the findings are compared to published data of six glaciers in the Alps, Northern Europe, the United States and Bolivia.

The detailed investigations in Austria include the mass balances of Hintereisferner (HEF), Kesselwandferner (KWF) and Vernagtferner (VF) in the Ötztal Alps; Jamtalferner (JAM) in Silvretta; Übergossene Alm on Hochkönig (HK) in the Salzburg Limestone Alps; and Stubacher Sonnblickkees (SSK) in Hohe Tauern. These data are compared in Sect. 4.2 to published data of Griesgletscher (GG, Funk et al., 1996), Gulkana Glacier (GU, Cox and March, 2004), Lemon Creek glacier (LC, Miller and Pelto, 1999), South Cascade glacier (SC, Krimmel, 1999), Storbreen (SB, Andreassen, 1999), Storglaciären (SG, Zemp et al., 2010), and Zongo glacier (ZG, Soruco et al., 2009).

2 Methods

Glacier mass balance measurements began at the end of the 19th century (Hess, 1904). The concepts and techniques were further developed in the second half of the century (Ahlmann, 1948; Finsterwalder, 1953). During this period, the geodetic method was often used as a simple way to estimate volume changes of glaciers over multi-annual time scales as an independent control (Hoinkes, 1970). In fact, using the geodetic method in this way was complicated by two reasons. First, in many cases the accuracy of photogrammetric maps of the firn area was low due to the lack of contrast on white surfaces of the orthophotos. Second, the density of the surface layer was known only rarely then (Hoinkes, 1970), and today.

2.1 Geodetic method

The geodetic mass balance is calculated from the volume change derived from topographic data. This alone is not sufficient since estimates of the densities of the lost or gained volumes are also necessary. Two digital elevation models (DEMs) are acquired at different dates t_1 and t_2, usually at the end of of the ablation period. The length of the experimental time period $\Delta t = t_2 - t_1$ can vary from as little as one year to many decades. The volume change ΔV in the period Δt is then calculated for the entire glacier either from the contour lines of elevation as described by Lang and Patzelt (1971) or with a raster method as performed by Funk et al. (1996). The multiplication of the volume change ΔV with the mean density ρ results in the mass balance B_{geo} within this period.

$$B_{\mathrm{geo}} = \Delta V * \rho \tag{1}$$

In most studies, the density ρ is estimated, not measured. The density of the surface layer of a glacier varies with time and space and ranges between 100 kg m^{-3} and 917 kg m^{-3}. Most assumes mean densities fall between 800 kg m^{-3} and 900 kg m^{-3}. The mean density of ΔV changes with a sign opposite that of the mass balance, as ice gained by accumulation has a lower density than ice lost by ablation. In this study, a density of 850 kg m^{-3} was assumed to account for long term volume loss in the accumulation area, where the mean density is lower than at the glacier tongue.

TCD
4, 1151–1194, 2010

By definition, the specific mass balance b is the mass balance B divided by the glacier area A. If the time period between the acquisition of the DEMs is more than a few years, the glacier area typically changes. In this study, the specific geodetic mass balance b_{geo} is calculated by dividing the mass balance by the larger glacier area A, in case of glacial recession A at the time t_1.

$$B_{geo} = b_{geo} * A_{t1} \tag{2}$$

The sketch of the geodetic method in Fig. 1 shows a cross section of one glacier at the dates t_1 and t_2. The glacier is composed of ice, firn and snow; materials with different densities are indicated by the color gradient from white (low density) to blue (high density). The glacier surface layer in this example consists of snow in the high elevations and ice below. The elevation change $h_2 - h_1$ between the acquisition dates of the DEMs is calculated on a regular grid and shown for one transect in the lower part of Fig. 1. In the example shown in the sketch, the elevation changes are related to the surplus of snow accumulation in the upper part of the glacier and internal as well as surface ablation in the lower parts of the glacier. The density of the snow layer changes between t_1 and t_2. The sketch is simplified, and does not show that the ice flow transports mass from the upper parts of the glacier towards the tongue. Thus for the specific grid points, the elevation change is always the algebraic sum of mass balance and ice flow. For the total glacier area, a common assumption is that ice flow does not alter the total mass of a glacier, and therefore changes of the glacier volume are related to mass changes only.

2.2 Glaciological method

The direct or glaciological method to measure mass balance is based on in situ determination of accumulation and ablation for the mass balance year (Hoinkes, 1970; Braithwaite, 2002). For all Austrian test glaciers analyzed in this study, the mass balance is determined within the hydrological year from 1 October and 30 September (a fixed date system). The sketch in Fig. 2 shows the mass balance measurements with

TCD
4, 1151–1194, 2010

snow pits in the accumulation area and stakes in the ablation area. Ablation stakes are drilled in the ice and read at the end of the hydrological year. The seasonal snow cover in the ablation area at the 30 September is included in the balance as mass gain. The amount of accumulation is determined by digging several snow pits and measuring the thickness and the density of the snow cover gained since the 1 October of the previous year. To do so, a clear seasonal horizon observable each year in the snow cover. The spatial distribution of the accumulation is mapped by snow probing, if the seasonal horizon is hard enough, or by assuming a typical spatial pattern of snow patches which is found by multi-annual observation of melt patterns.

Interpolation from the measured data is performed manually by constructing contour lines of equal mass balance, in most cases including additional observations or information such as avalanches or ice exposure time. For the surface layer, the density variations are indicated by the color gradient of the glacier from white to blue in Fig. 2 and are measured in situ.

The direct or glaciological mass balance is a surface mass balance, as it does not include mass change below the surface, that is, intra- or subglacial melt or accumulation. The direct mass balance is defined in the vertical direction, so that it is calculated for the glacier area projected on a map and not the real surface area. Figure 2 shows that the same distance n in map projection can correspond to different distances m and n at the glacier surface. Thus the surface area of steep parts of the glacier is larger than the area projected on the map, a problem which is currently neglected in most mass balance calculations.

3 Test sites and data

Six Austrian glaciers were selected as test sites for the comparison of direct and geodetic mass balance data (Table 1, Figs. 3 and 4): HEF, VF and KWF in Ötztal Alps, JAM in Silvretta, SSK in Hohe Tauern, and HK in the Salzburg Northern Limestone Alps. For all these glaciers, long term direct and geodetic data are available. For all these glaciers,

TCD
4, 1151–1194, 2010

surface elevation data for 1969 and 1997 to 2002 are available from the first and second glacier inventories (Patzelt, 1978; Lambrecht and Kuhn, 2007; Gross, 1987). For HEF, KWF, VF and JAM the third Austrian glacier inventory (Abermann et al., 2009) also provides DEMs dating between 2004 and 2006. For HEF, four more DEMs were acquired in 1953, 1964, 1967 and 1979 (Kuhn, 1979). One DEM was acquired on KWF in 1971. All available DEMs are summarized in Table 2.

Hintereisferner (HEF) in Ötztal Alps is the largest test glacier with an area of with 9.5 km^2 and has a maximum elevation of 3710 m a.s.l. The valley glacier has a pronounced tongue and therefore a large ablation area with bare ice. HEF has the most negative mass balance of the test glaciers. Since the beginning of the mass balance measurements in 1952/1953 the firn cover dropped significantly (Lang and Patzelt, 1971; Fischer and Markl, 2008). Since 1952/1953, many different methods of evaluating the annual mass balances have been used, so it was necessary to homogenize the whole data set (Fischer, 2010). The coordinate system used for DEMs on Hintereisferner changed between 1967 and 1969 from the Munich system to the Austrian Gauss Krüger System. The horizontal deviation between these coordinates is up to 4 m. At the moment, as accurate transformation parameters are not available, this might have an effect on the geodetic mass balance between 1967 and 1969.

The adjacent Kesselwandferner (KWF) has about half of the area of Hintereisferner and has a smaller and higher ablation area. The mass balance of KWF, which has also been measured since 1952/1953, is therefore less negative than the mass balance of HEF. As shown by Kuhn et al. (1985), Hintereisferner and Kesselwandferner respond differently to climate variations.

The mass balance of the nearby Vernagtferner (VF) has been measured since 1964/1965 (Reinwarth and Escher-Vetter, 1999). The size of VF is similar to that of HEF, but the glacier type and topography differ. Vernagtferner also experienced a strong recession of the firn cover since 1964/1965.

Übergossene Alm (HK) is a plateau glacier situated in the northeastern corner of Fig. 3 and located entirely below 3000 m. The mass balance was measured by

Goldberger (1986) between 1965 and 1996. The mass balance series ended in 1996, six years before 2002, when the the second DEM was acquired. Since the years from 1996 to 2002 brought further mass loss on HK, the direct data is a low estimate for the mass loss between 1969 and 2002.

The mass balance of Jamtalferner in Silvretta has been measured since 1989 (Fischer and Markl, 2008). The glacier is located between 2480 m a.s.l. and 3160 m a.s.l. The low elevation is explained by the large amount of accumulation relative to HEF, VF and KWF. The size of JAM is similar to KWF.

Stubacher Sonnblickkees in Hohe Tauern has been measured since 1959 (Slupetzky, 1999). The Stubacher Sonnblickkees is a plateau glacier. It has about the same size as Übergossene Alm, but spans a wider range of elevations.

As indicated in Table 2, the DEMs were compiled with different techniques. Until 2003, the DEMS were compiled with terrestrial or airborne photogrammetry. Up to 1969, the DEMs were compiled with terrestrial photogrammetry. The DEMs used in this study dating from 2004 and later were acquired with airborne laser scanning. Improvements in methods for both the direct and the geodetic data have resulted in increasing accuracy over time.

4 Results for six Austrian glaciers

The glaciers show generally negative mass balances except between 1965 and 1969 and around 1980 (Fig. 5). The mean annual geodetic mass balance for all 19 periods of HEF, KWF, JAM, VF and SSK between 1953 and 2006 is −0.5 m w.e./year (Table 3). The mean difference $b_{geo} - b_{direct}$ between the direct and the geodetic data is −0.6 m w.e.; the maximum is 5.6 m w.e., and the minimum −7.0 m w.e. The average length of the time periods is 16.3 years, the minimum is 2 years and the maximum 53 years. On HEF, the geodetic mass balance differs from the direct by −7.4 m w.e. for the total period (53 years). The geodetic mass balance for HEF gives an average of 0.14 m w.e. per year less than a medium year with direct data. On KWF (37 years),

TCD
4, 1151–1194, 2010

the geodetic mass balance differs from the direct by −2.2 m w.e. On SSK, JAM and VF, the geodetic mass balance is greater than the direct, the difference is +0.3 m w.e. for JAM, +4.7 m w.e. for SSK and +0.6 m w.e. for VF (37 years). For 9 time periods, the geodetic mass balance is greater than the direct, for 10 periods the direct mass balance is greater and in one period, the mass balances are equal.

The time series of the direct mass balance of HK ended in 1996, before the acquisition of the second DEM in 2002. The cumulative direct mass balance from 1969 to 1996 was −10.8 m; the geodetic mass balance from 1969 to 2002 was −7.7 m (Table 3). Since the direct mass balance between 1997 and 2002 can be assumed to be negative, the direct mass balance is more negative than the geodetic mass balance by more than 3.1 m.

Figure 5 shows the cumulative direct mass balance and the cumulative geodetic mass balance for HEF, KWF, JAM, VF, SSK and HK. For the glacier with the most negative mass balance, HEF, the cumulative geodetic mass balance is more negative than the direct. After years with positive mass balances (1965 to 1969 and 1977 to 1979), the geodetic mass balance (dots in Fig. 5) comes closer to the direct mass balance curve. The deviation of the curves increases with time and reaches its maximum in 2006 after several years with strong volume losses.

The mass balance of KWF for the observation period is the least negative of the investigated glaciers. From 1969 to 1971, the geodetic mass balance is positive, whereas the directly measured mass balance is close to 0. The geodetic mass balance is less negative than the direct mass balance for all subperiods. Between the 1971 DEM and the 1997 DEM the tongue of KWF advanced approximately 600 m, then melted again. During the advance,the surface was very rough. Thus the assumed density of 900 kg m^{-3} is a poor estimate of the true density, since the crevasses included in the glacier volume of 1971 contain a lot of air (Figs. 6 and 10).

The adjacent glaciers VF and KWF were surveyed geodetically during the same periods: 1969 to 1997 and 1997 to 2006. From 1969 to 1997, KWF (−2.9 m w.e.) and VF (−2.6 m w.e.) show a quite similar geodetic mass balance, but the direct mass balance of VF (−8.2 m w.e.) is about 4 times the direct mass balance of KWF (−1.7 m w.e.). At KWF, where the mass balance was close to zero, the difference between the geodetic and direct mass balance is small. On VF, where the mass balance was more negative, the differences between the direct and geodetic mass balance were larger. The observation period of SSK is comparable to that of VF and KWF (1969 to 1998); there the geodetic mass balance differs from the direct mass balance by 4.7 m.

For JAM, the agreement between the geodetic and the direct data is very good for all periods. The glacier shows high accumulation rates, and is located in elevations below 3300 m. The glacier tongue is small, and the firn cover shrank greatly after 2003.

The difference between the direct and the geodetic mass balance is analyzed over all 19 periods to find if these differences also depend on the mass balance itself. Between 1965 and 1985, the direct mass balances b_{direct} of HEF, KWF, JAM, VF, HK and SSK were more positive than before and after these years (Fig. 7). The geodetic data of this period are even more positive than the direct data. A possible explanation for that is seasonal snow cover on the glacier at the time of the second DEM, and its misinterpretation as less ice melt. From 1997 to 2006, most glaciers had strongly negative mass balances. During this time period, the geodetic mass balances are more negative than the direct data. This is the result of basal melt and densification processes as well as seasonal snow cover at the time of the first DEM.

4.1 Error analysis

The error inherent in the geodetic and direct data must be accounted for in order to accurately compare the two methods. Fountain and Vecchia (1999) and Kuhn et al. (1999) estimated the accuracy of the direct mass balance as 0.1 m w.e./year.

The accuracy of the geodetic mass balance depends on the accuracy of the two DEMs and the accuracy of the density of the surface layer. For Svartisen ice cap, Rolstad (2009) analyzed the the geodetic mass balance and found an accuracy of ±0.9 m w.e. to 2.2 m w.e. This geostatistical approach was applied to two time periods.

This article explores the accuracy of the geodetic mass balance in detail by examining simple, process-oriented case studies.

4.1.1 Accuracy of the DEMs

The DEMs used here are acquired with different techniques listed in the order of increasing accuracy (Table 2):

TERRESTRIAL PHOTOGRAMMETRY. The topographic data before 1969 analyzed in this study were derived from old maps which are themselves based on terrestrial photogrammetry. The DEMs were digitized from the contour lines of orthorectified historical maps and processed to a raster with 5 m grid size using the Topo2raster tool of the ARCGis Software. The horizontal RMS errors of the rectified maps caused by drawing inaccuracies, changes of the map paper and coregistration are ±1 m. The accuracy of this elevation data depends on the imaging geometry and the location of the station points. Haggrén et al. (2007) reanalyzed the terrestrial photogrammetry data of Hochjochferner dating from 1907. From the comparison of the map of 1907 to the reanalyzed DEM they concluded that the terrestrial photogrammetric data has an accuracy of ±10 m. The tacheometrically surveyed glacier tongue showed an error of ±1–2 m.

AIRBORNE PHOTOGRAMMETRY. According to Würländer and Eder (1998), the accuracy of the airborne photogrammetric data used in this study is better than ±0.71 m. Lang and Patzelt (1971), reported that the accuracy of photogrammetric DEMs depends on the contrast of the images. As reported by Abermann et al. (2007), local errors can be significantly higher due to oversaturation or shadows in photogrammetric images. Errors in the photogrammetric DEM of Kesselwandferner acquired in 1997 are >10 m (Abermann et al., 2007). All three glacier inventory datasets are available digitally, thus no additional referencing errors occurred during the digitalization of maps.

AIRBORNE LASER SCANNING. According to (Høgda et al., 2007), the airborne laser scanning (LIDAR) technology allows the acquisition of DEMs with a vertical precision of a few cm independent of the texture and the contrast on the glacier surface . Geist and Stötter (2007) investigated LIDAR data on Hintereisferner and Kesselwandferner and found a relative vertical accuracy of 0.3 m and a relative horizontal accuracy of 1.0 m. The point distance of LIDAR systems is 0.1 m to 1.4 m, the pixel size 1 m to 2.5 m.

For all kinds of digital topographic data, the absolute coregistration, the resolution and the pixel sizes affect the vertical accuracy. The absolute horizontal accuracies of DEMs and coregistered historical data also depend on the availability of referenced tie points. Near Hintereisferner and Kesselwandferner, a net of geodetic fix points installed from 1893 onwards ensured high accuracy. Figure 8a shows an example where a change in the grid size causes a virtual change Δz in elevation. Since alpine glaciers tend to be inclined over the surface, this effect does not necessarily even out over the total glacier area. Historical topographic data use different, and sometimes even local, coordinate systems than contemporary DEMs. Thus coordinate transformations with appropriate parameters are necessary to avoid horizontal errors. Using standard transformation parameters, the horizontal error of the transformation between UTM WGS84 32 N and Gauss-Krüger coordinates is up to several meters on HEF. The older maps of HEF are compiled in a local coordinate system with horizontal deviations of up to 4 m from the coordinates of the new maps (Abermann et al., 2007). If the slope is inclined by 45°, a horizontal error Δx causes a vertical error $\Delta z = \Delta x$ (Fig. 8b).

4.1.2 Seasonal snow cover

Seasonal snow cover is a potential source of error for the geodetic method (Fig. 9). If seasonal snow cover is misinterpreted as ice, the glacier volume is overestimated. Depending on the time of the snow fall event, this results in either under- or overestimation of the geodetic mass balance. When no seasonal snow covers the glacier, the measured thickness change h_m corresponds to the ice thickness change b_geo (Fig. 9a). If the snow cover occurs during the acquisition of the first DEM (Fig. 9b), the ice thickness change is overestimated by $+\Delta h$. If the snow covers the glacier during the acquisition of the second DEM, the ice thickness change is underestimated by $-\Delta h$.

If one DEM within a time series t_1, t_2 and t_3 is affected by seasonal snow cover at t_2, the error balances out: ΔV_{t1t2} is for example too high and ΔV_{t2t3} too low. If the snow cover occurs at t_1 or t_3 the error extends over the entire period. Since the DEMs of 1969 are very likely affected by seasonal snow layers, the geodetic mass balances using the 1969 data as the second DEM are underestimated. The geodetic mass loss from 1969 to 1997 is likely to be overestimated, as is evident in Fig. 7.

The density of the snow layer (white in Fig. 9) ranges from $100\,\mathrm{kg\,m^{-3}}$ to about $500\,\mathrm{kg\,m^{-3}}$, the density of ice (blue in Fig. 9) is assumed to be $900\,\mathrm{kg\,m^{-3}}$. Thus within the period of the DEM acquisitions, the density of the surface layer can change by up to $800\,\mathrm{kg\,m^{-3}}$. A short example demonstrates the possible error of b_{geo}: If a thickness change of 1 m of snow cover with a density of $500\,\mathrm{kg\,m^{-3}}$ (0.5 m w.e.) is interpreted as change of 1 m ice (0.9 m w.e.), the error is 0.4 m w.e. The typical height of the winter snow cover on HEF ranges from 1–2 m on the glacier tongue to 5–7 m at the deepest snow pit. On Hallstätter glacier, winter snow cover with heights locally exceeding 10 m was observed. Snows in autumn (before 30 September) were observed to reach more than two meters on Hintereisferner and Hallstätter glacier; in August, snow cover may reach a height of 1.5 m. Thus, seasonal snow cover can result in errors of the same magnitude as the measured geodetic mass balance.

4.1.3 Density changes

Apart from the short term changes of surface layer density caused by seasonal snow cover, the mean density of the surface layer also changed during the last decades as a results of strongly negative mass balances. The reduction of firn cover and the densification of firn layers and crevasses result in a misinterpretation of volume changes as mass changes (Fig. 12). If the mean density of snow, firn and ice decreases (Fig. 12a), the glacier surface drops without mass change. Another mechanism for a reduction in surface height without mass change is also refreezing of melt water in a cold firn layer. Assuming the conservation of mass, fewer and smaller crevasses result in a lowering of the glacier surface (Fig. 12b). If the spatial resolution of the DEMs is high, crevasses can be visible if they are not covered with snow. In earlier datasets with lower resolution, crevasses are not included (Fig. 12c).

Discussion Paper | Discussion Paper | Discussion Paper | Discussion Paper |

TCD

4, 1151–1194, 2010

Direct and geodetic mass balances on a multi-annual time scale

A. Fischer

All Austrian glaciers experienced high amounts of accumulation in the 1960s and 1970s. Thus the mean density of the surface layer in the firn areas was lower than during the following years with strong negative mass balances. In 2003, even the highest glaciers in Austria lost most of their firn cover. Measurements on HEF showed a density of the surface layer of 800 kg m^{-3} at 3000 m. Figure 11 is an example for the changes of the firn area at HEF. Between the 1969 and 1997 and during the years of strong negative mass balances beginning with 2003, the change of the density of the surface layer was observed.

A short example shows the possible contribution of the densification to the total volume change of Austrian Alpine glaciers. Ambach (1995) surveyed a 20 m deep firn pit on KWF and observed densities from 640 kg m^{-3} to 840 kg m^{-3}. To estimate the effect of density changes within a firn column on the volume of the column, we calculate a small example. Assuming a firn column with 10 m height and a mean density of 750 kg m^{-3}. A change of the mean density to 800 kg m^{-3} results in a thickness change of 0.6 m. Another example for a density change without mass change could be the densification of the top layer in the firn area. Assuming a snow layer with a height of 1 m and a density of 200 kg m^{-3}, the thickness of this layer can decrease by 0.5 m when the density increases to 400 kg m^{-3}.

Thus thickness changes resulting from densification are of the same order of magnitude as the mean annual thickness change of Austrian glaciers between 1969 and 1997 (Lambrecht and Kuhn, 2007).

Whereas the densification process plays a role mainly in the firn area, crevasses occur at all altitudes. Since the 1980s, the ice flow velocities reduced from over 100 m per year at several glaciers to just several m per year. Thus fewer and smaller crevasses are observed (Figs. 12b and 10). This effect alters the mean density of the glacier even in the ablation area. Currently neither estimates nor measurements of the volume change caused by crevasse-related changes.

A problem which appeared with very precise DEM data with high spatial and vertical resolution is the imaging of crevasse volume. Photogrammetric maps or DEMs or tacheometric surveys rarely mapped crevasses. LIDAR data maps crevasses, if they are not covered with snow. If crevasses appear on newer DEMs, but not on the older ones, the volume loss is overestimated. If crevasses are covered with snow on the first LIDAR image, but not on the second LIDAR image, crevasse volume is included in volume change. (Fig. 12c).

4.1.4 Basal or internal melt

The geodetic mass balance includes basal or internal melt if the effects propagate to the glacier surface. The total change in surface elevation Δh_s results from internal Δh_i and basal ice thickness changes Δh_b (Fig. 14). In contrast to that, the direct mass balance is a surface mass balance and includes Δh_s only.

The development of Mittelbergferner (MBF) in Ötztal Alps (Fig. 3) shows that locally the basal mass balance can contribute significantly to the volume change at the surface (Fig. 14). At an altitude of about 2500 m a.s.l. near the glacier margin radial crevasses are surrounding a zone with fast subsidence (Fig. 13). The surface elevation dropped by 82 m in 9 years. The annual ablation is less than 9.1 m. The ice thickness above the subsidence zone is still 70 to 100 m; the ice flow velocity is most likely not zero. Therefore, the reason for the quick surface drop in this zone can only be basal melt. The high amounts of basal melt can be explained by two large melt water streams which join underneath the subsidence zone.

Wiesenegger and Slupetzky (2009) made similar observations on Stubacher Sonnblickkees. Detailed measurements to quantify the effect for SSK and HEF are ongoing.

4.2 Comparison of the results to published data

The published data of Griesgletscher (Funk et al., 1996), Gulkana glacier (Cox and March, 2004), Storglaciären (Zemp et al., 2010), South Cascade Glacier (Krimmel, 1999), Lemon Creek glacier (Miller and Pelto, 1999), Storbreen (Andreassen, 1999)

TCD
4, 1151–1194, 2010

and Zongo glacier (Soruco et al., 2009) include the geodetic and direct mass balance data of 26 time periods between 1940 and 2006. The average length of the periods is 18.2 years (Table 4). The longest period lasts 57 years, the shortest 2 years. The temporal distribution of the data is similar to that of the Austrian data. Where only the volume change without information on the mass balance or on the density of the surface layer was provided, the geodetic mass balance was calculated assuming a mean density of 850 kg m^{-3}. The glaciers are located in different regions and different local climates, but the average annual geodetic mass balance is −0.4 m w.e./year and thus similar to the mean of the Austrian data (−0.5 m w.e./year).

The mean difference is −0.4 m w.e., the maximum difference 3.6 m w.e. and the minimum difference −7.2 m w.e. Thus these data are in accordance with the data of the six the Austrian glaciers.

The data of Storbreen confirm the finding that a longer measurement period length does not automatically result in more agreement between the geodetic and the direct mass balances (Fig. 15). Just like the Austrian glaciers, Storglacieren, South Cascade and Lemon Creek show higher differences during periods with strongly negative mass balances. This is not the case for Storbreen and Griesgletscher.

Figure 16 is a plot of the geodetic vs. the direct mass balance. As stated by Cogley (2009), no common trend for all glaciers is obvious. Some glaciers do show trends, which are related to the specific properties of the glacier. For example on HEF the geodetic mass balance is more negative than other mass balances. The more negative the mass balances, the greater the differences. This is caused by glacier topography: melt water from the entire glacier area flows underneath the pronounced glacier tongue of this valley glacier. On Jamtalferner, the difference between direct and geodetic data shows nearly no trend, which could also be caused by compensation of different processes. Lemon Creek shows a trend opposite to that of HEF: the geodetic mass balances are increasingly less negative than the direct.

The accuracy of the direct data is ±0.01 m w.e./year. Assuming a period of 10 years, the mean accuracy of the geodetic method on Austrian Alpine glaciers results

TCD
4, 1151–1194, 2010

densification (±0.1 m w.e./year), seasonal snow cover (±0.1 m w.e./year) and basal melt (0.5 m w.e./year), as well as the accuracy of the DEMs. Terrestrial photogrammetric DEMs with good coregistration in our example show errors of 1.0 m/year; LIDAR DEMs have errors of 0.001 m/year for the 10 year period. The uncertainty of at least $\pm 50\,\mathrm{kg\,m^{-3}}$ in the mean density adds 10% error to the geodetic mass balance which then is 1.0 m w.e./year and 0.001 m w.e./year, respectively. Thus the cumulative error of the geodetic mass balance is 2.7 m w.e./year for two terrestrial photogrammetric DEMs, and 0.702 m w.e./year for two LIDAR DEMs. For historical data, the errors of the DEMs dominate the total error, whereas for LIDAR data glaciological processes dominate. The time period for the calculation of geodetic data should be chosen in relation to the total mass balance to ensure that the mass balance within this period is significantly larger than the error values.

5 Conclusions

The direct and the geodetic mass balances differ systematically. The geodetic data include basal and internal mass changes, which are shown to contribute significantly to the total mass change on the tongue of Mittelbergferner. The mean density of the volume changes varies in time and space. The best agreement between the geodetic and the direct mass balance therefore is expected for glaciers in equilibrium. The differences increase with increasing negative mass balances for most investigated glaciers. The differences show trends likely related to glacier state and glacier type. The investigated Austrian glaciers with less negative mass balances receive a higher amount of accumulation and show smaller differences between geodetic and direct data. The largest differences are observed during periods with strong negative mass balances, when the basal melt caused by the subglacial melt water streams is expected to be high.

The accuracy of the geodetic data in Alpine regions ranges from 2.7 m for terrestrial photogrammetric data and 0.7 m for the LIDAR data. Errors in the coregistration,

TCD
4, 1151–1194, 2010

different pixel sizes of the DEMs, shadows and oversaturation of photogrammetric images increase the total error.

The comparison of the difference between the geodetic and the direct method with the length of the observation period showed that longer observation periods do not necessarily reduce the difference between the geodetic and the direct mass balance.

In summary, the results show that the geodetic and the direct glaciological method are not only different ways to measure the same parameter, but map different processes. The inclusion of intra- and subglacial melt is a clear advantage for the geodetic data to estimate the contribution of glaciers to global sea level rise. On the other hand, the geodetic method can be easily biased by seasonal snow cover and missing information about density. The direct mass balance measures the surface mass balance with high accuracy and high temporal resolution, whereas the temporal resolution of the geodetic data is limited by the errors of up to 2.7 m w.e. During periods of high melt rates, the reduction and densification of firn cover biases the geodetic mass balance.

In conclusion, direct and geodetic mass balance are both valuable tools for different applications. They both contain specific, but different information on glacier mass balance. A mix of direct and geodetic data should be handled with caution. To avoid biases in long time series of mass balance data, the method of measurement should remain constant.

Acknowledgements. This work was funded by the Herta-Firnberg Grant ZFT 3290 of the Austrian Science Foundation. The field work on Hintereisferner, Kesselwandferner, and Jamtalferner and the acquisition of the glacier inventories of 1969 and 1998 were supported by the Hydrographical survey of the federal government of Tyrol and the Commission of Geophysics of the Austrian Academy of Sciences. The DEMs 2004 to 2006 for the third Austrian glacier inventory were provided by the Federal government of Tyrol. The Tyrolean Science Foundation supported a pilot study for the third glacier inventory.

References

Abermann, J., Schneider, H., and Lambrecht, A.: Analysis of surface elevation changes on Kesselwand glacier. comparison of different methods, Z. Gletscherk. Glazialgeol., 41, 147–167, 2007. 1163, 1164

Abermann, J., Lambrecht, A., Fischer, A., and Kuhn, M.: Quantifying changes and trends in glacier area and volume in the Austrian Ötztal Alps (1969–1997–2006), The Cryosphere, 3, 205–215, doi:10.5194/tc-3-205-2009, 2009. 1159

Ahlmann, H.: Glaciological Research on the North Atlantic Coasts, no. 1 in Royal Geographical Society, Research Series, 1948. 1156

Ambach, W.: Depth profiles of effective viscosities of temperate firn following from strain rate measurements at two firn pits (Kesselwandferner, Oetztal Alps, 1967–1989), http://www.ingentaconnect.com/content/els/0165232x/1995/00000023/00000003/art00017, last access: 22 July 2010, Cold Reg. Sci. Technol., 23(8), 257–264, 1995. 1166

Andreassen, L.: Comparing traditional mass balance measurements with long term volume change extracted from topographical Maps: a case study for Storbreen glacier in Jotumheimen, Norway, for the period 1940–1997, Geogr. Ann. A, 81A, 467–475, 1999. 1155, 1167, 1178

Braithwaite, R. J.: Glacier mass balance: the first 50 years of international monitoring, http://ppg.sagepub.com/cgi/content/abstract/26/1/76, last access: 22 July 2010, Prog Phys. Geog., 26, 76–95, doi:10.1191/0309133302pp326ra, 2002. 1157

Cogley, J.: Geodetic and direct mass-balance measurements: comparison and joint analysis, Ann. Glaciol., 50(50), 96–100, 2009. 1154, 1168

Cox, L. H. and March, R. S.: Comparison of geodetic and glaciological mass-balance techniques, Gulkana Glacier, Alaska, USA, http://www.ingentaconnect.com/content/igsoc/jog/2004/00000050/00000170/art00006, last access: 22 July 2010, J. Glaciol., 50, 363–370(8), doi:10.3189/172756504781829855, 2004. 1154, 1155, 1167, 1178

Finsterwalder, R.: Die zahlenmäßige Erfassung des Gletscherrückgangs an Ostalpengletschern, Z. Gletscherk. Glazialgeol., 2, 189–239, 1953. 1156

Fischer, A.: Glaciers and climate change: Interpretation of 50 years of direct mass balance of Hintereisferner, Global Planet. Change, http://www.sciencedirect.com/science/article/B6VF0-4XSJVPY-1/2/fc79744605283942a6d4eb85bad3daf2, last access: 22 July 2010, 71, 13–26, doi:10.1016/j.gloplacha.2009.11.014, 2010. 1159

Fischer, A. and Markl, G.: Mass balance measurements on Hintereisferner, Kesselwandferner, and Jamtalferner 2003 to 2006. database and results, Z. Gletscherk.. Glazialgeol., 42, 47–83, 2008. 1159, 1160

Fountain, A. G. and Vecchia, A.: How many stakes are required to measure the mass balance of a glacier?, http://www.jstor.org/stable/521494, last access: 22 July 2010, Geogr. Ann. A, 81, 563–573, 1999. 1162

Funk, M., Morelli, R., and Stahel, W.: Mass balance of Griesgletscher 1961–1995: different methods of determination, Z. Gletscherk. Glazialgeol., 33(1), 41–55, 1996. 1155, 1156, 1167, 1178

Geist, T. and Stötter, J.: Documentation of glacier surface elevation change with multitemporal airborne laser scanner data – case study: Hintereisferner and Kesselwandferner, Tyrol, Austria, Z. Gletscherk. Glazialgeol., 41, 77–106, 2007.. 1154, 1163

Goldberger, J.: Gletscherhaushalt und klimatische Umwelt des Hochköniggletschers 1965–1975, Wissenschaftliche Alpenvereinshefte, 28, 1986. 1160

Gross, G.: Der Flächenverlust der Gletscher in Österreich 1850–1920–1969, Z. Gletscherk. Glazialgeol., 23, 131–141, 1987. 1159

Haggrén, C., Mayer, C., Nuikka, M., Braun, L., Rentsch, H., and Peipe, J.: Processing of old terrestrial photography for verifying the 1907 digital elevation model of Hochjochferner glacier, Z. Gletscherk. Glazialgeol., 41, 29–35, 2007. 1163

Hess, H.: Die Gletscher, F. Vieweg and Son, Braunschweig, Germany, 1904. 1155

Høgda, K., Geist, T., and Jackson, M.: Comparison of digital elevation models of Engabreen glacier, Z. Gletscherk. Glazialgeol., 41, 185–204, 2007. 1163

Hoinkes, H.: Methoden und Möglichkeiten von Massenhaushaltsstudien auf Gletschern, Z. Gletscherk. Glazialgeol., 6, 37–90, 1970. 1153, 1156, 1157

Huss, M., Bauder, A., and Funk, M.: Homogenization of long-term mass-balance time series, http://www.ingentaconnect.com/content/igsoc/agl/2009/00000050/00000050/art00028, last access: 22 July 2010, Ann. Glaciol., 50(9), 198–206, doi:10.3189/172756409787769627, 2009. 1154

Jarvis, A., Reuter, H., Nelson, A., and Guevara, E.: Hole-filled seamless SRTM data V3, International Centre for Tropical Agriculture (CIAT), http://srtm.csi.cgiar.org, last access: 1 May 2006. 1181

Kaser, G., Cogley, J., Dyurgerov, M., Meier, M., and Ohmura, A.: Mass balance of glaciers and ice caps: consensus estimates for 1961–2004, Geophys. Res. Lett., 33, L19501, doi:10.1029/2006GL027511, 2006. 1153

Krimmel, R. M.: Analysis of difference between direct and geodetic mass balance measurements at South Cascade Glacier, Washington, Geogr. Ann. A, 81(4), 653–658, 1999. 1154, 1155, 1167, 1178

Kuhn, M.: Begleitworte zur Karte des Hintereisferners 1979, 1:10 000, Z. Gletscherk. Glazialgeol., 16, 117–124, 1979. 1159

Kuhn, M., Markl, G., Kaser, G., Nickus, U., Obleitner, F., and Schneider, H.: Fluctuations of climate and mass balance: different responses of two adjacent glaciers, Z. Gletscherk. Glazialgeol., 21, 409–416, 1985. 1159

Kuhn, M., Dreiseitl, E., Hofinger, S., Markl, G., Span, N., and Kaser, G.: Measurements and models of the mass balance of Hintereisferner, Geogr. Ann. A, 81A, 659–670, 1999. 1154, 1162

Lambrecht, A. and Kuhn, M.: Glacier changes in the Austrian Alps during the last three decades, derived from the new Austrian glacier inventory, Ann. Glaciol., 46, 177–184, 2007. 1159, 1166

Lang, H. and Patzelt, G.: Die Volumenänderungen des Hintereisferners (Ötztaler Alpen) im Vergleich zur Massenänderung im Zeitraum 1953–64, Z. Gletscherk. Glazialgeol., 7(1–2), 229–238, 1971. 1154, 1156, 1159, 1163

Lemke, P., Ren, J., Alley, R., Allison, I., Carrasco, J., Flato, G., Fujii, Y., Kaser, G., Mote, P., Thomas, R., and Zhang, T.: Climate Change: The Physical Science Basis, Contribution of Working Group I to the Fourth Assessment Report of the IntergovernmentalPanel on Climate Change, chap. Observations: Changes in Snow, Ice and Frozen Ground, Cambridge University Press, Cambridge, Uk and New York, 2007. 1153

Miller, M. M. and Pelto, M. S.: Mass Balance Measurements on the Lemon Creek Glacier, Juneau Icefield, Alaska 1953–1998, http://www.jstor.org/stable/521505, last access: 22 July 2010, Geogr. Ann. A, 81, 671–681, 1999. 1155, 1167, 1178

Patzelt, G.: The Austrian glacier inventory: status and first results, IAHS-AISH P., 26, 181–184, 1978. 1159

Reinwarth, O. and Escher-Vetter, H.: Mass balance of Vernagtferner, Austria, from 1964/1965 to 1996/1997: results for three sections and the entire glacier, Geogr. Ann. A, 81A, 743–751, doi:10.1111/j.0435-3676.1999.00102.x, 1999. 1159

Rolstad, C.: Spatially integrated geodetic glacier mass balance and its uncertainty based on geostatistical analysis: application to the western Svartisen ice cap, Norway, http://www.ingentaconnect.com/content/igsoc/jog/2009/00000055/00000192/art00009, last access: 22 July 2010, J. Glaciol., 55(15), 666–680, 2009. 1162

Slupetzky, H.: Programm "Wasser- und Eishaushaltsmessungen im Stubachtal" (Massenbilanzmessreihe vom Stubacher Sonnblickkees). Ergebnisbericht für 1992, Mitteilungsblatt des Hydrographischen Dienstes in Österreich, 70, 115–131, 1999. 1160

Soruco, A. V. C., Francou, B., Ribstein, P., Berger, T., Sicart, J., Wagnon, P., Arnaud, Y., Favier, V., and Lejeune, Y.: Mass balance of Glaciar Zongo, Bolivia, between 1956 and 2006, using glaciological, hydrological and geodetic methods, Ann. Glaciol., 50(50), 1–8, 2009. 1155, 1168, 1178

Thibert, E. and Vincent, C.: Best possible estimation of mass balance combining glaciological and geodetic methods, http://www.ingentaconnect.com/content/igsoc/agl/2009/00000050/00000050/art00016, last access: 22 July 2010, Ann. Glaciol., 50(7), 112–118, doi:10.3189/172756409787769546, 2009. 1154

Wiesenegger, H. and Slupetzky, H.: Der "Untere Eisboden See" – Entstehung eines neuen Gletschersees beim Stubacher Sonnblickkees, Mitteilungsblatt des Hydrographischen Dienstes in Österreich, 86, 49–63, 2009. 1167

Würländer, R. and Eder, K.: Leistungsfähigkeit aktueller photogrammetrischer Auswertemethoden zum Aufbau eines digitalen Gletscherkatasters, Z. Gletscherk. Glazialgeol., 35, 167–185, 1998. 1163

Zemp, M., Jansson, P., Homlund, P., Gärtner-Roer, I., Koblet, T., Thee, P., and Haeberli, W.: Comparison of glaciological and volumetric mass balance measurements at Storglaciären, Sweden, The Cryosphere Discuss., 4, 381–408, doi:10.5194/tcd-4-381-2010, 2010. 1154, 1155, 1167, 1178

Table 1. Austrian glaciers chosen for the comparison the direct and the geodetic method. abb … abbreviation, lon … longitide, lat … latitude, A … area, h_{max} maximum elevation in 1969 h_{min} minimum elevation 1969, last mb … last year of mass balance if not ongoing.

name	abb	lat N	lon E	A km^2	h_{max} m a.s.l.	h_{min} m a.s.l.	last mb year
Hintereisferner	HEF	46° 47.8′	10° 46.2′	9.502	3710	2390	
Jamtalferner	JAM	46° 51.7′	10° 09.7′	4.131	3160	2408	
Kesselwandferner	KWF	46° 50.3′	10° 47.9′	4.241	3490	2720	
Stubacher Sonnblickkees	SSK	47° 07.9′	12° 36.0′	1.772	3030	2500	
Übergossene Alm	HK	47° 25.6′	13° 03.7′	1.636	2845	2630	1996
Vernagtferner	VF	46° 52.6′	10° 49.0′	9.563	3628	2717	

TCD
4, 1151–1194, 2010

Table 2. Date and method of DEM acquisition at the test glaciers JAM, HEF, KWF, VF, SSK and HK. AL … airborne laser scanning, AP … airborne photogrammetry, TP … terrestrial photogrammetry.

glacier	AL	AP	AP	AP	TP	TP	TP
HEF	23 Aug/9 Sep 2006	12 Sep 1997	14/30 Aug 1979	Aug/Sep 1969	Sep 1967	20 Sep 1964	4 Sep 1953
HK		18 Sep 2002	Aug/Sep 1969				
JAM	Oct 2006	16 Sep 2002	Aug/Sep 1969				
KWF	23 Aug/9 Sep 2006	12 Sep 1997	18 Aug 1971	Aug/Sep 1969			
SSK		8 Aug 1998	Aug/Sep 1969				
VF	23 Aug/9 Sep 2006	12 Sep 1997	Aug/Sep 1969				

TCD

4, 1151–1194, 2010

Table 3. Results of the cumulative specific mass balance for the geodetic b_{geo} and the direct b_{direct} method. The numbers are rounded, the difference is calculated from the full values.

period year	b_{geo} m w.e.	b_{direct} m w.e.	Δb m w.e.
Hintereisferner (HEF)			
1953–1964	−7.5	−5.8	−1.7
1964–1967	1.3	1.3	0.0
1967–1969	−3.9	−0.1	−3.8
1969–1979	2.7	−1.8	4.5
1979–1991	−13.1	−8.0	−5.1
1991–1997	−4.4	−4.7	0.3
1997–2006	−10.1	−8.6	−1.5
total	−35.0	−27.7	−7.3
Kesselwandferner (KWF)			
1969–1971	0.6	0.0	0.6
1971–1997	−3.5	−1.7	−1.8
1997–2006	−5.0	−4.1	−0.9
total	−7.9	−5.8	−2.1
Jamtalferner (JAM)			
1996–2002	−2.0	−2.6	0.6
2002–2006	−5.0	−4.7	−0.3
total	−7.0	−7.3	0.3
Stubacher Sonnblickkees (SSK)			
1969–1998	−3.5	−8.2	4.7
Übergossene Alm, Hochkönig (HK)			
1969–1995		−10.8	
1969–2002	−7.7		
Vernagtferner (VF)			
1969–1997	−2.6	−8.2	5.6
1997–2006	−10.9	−5.8	−5.1
total	−13.5	−14.0	0.5

Table 4. Results of the cumulative specific mass balance for the geodetic b_{geo} and the direct b_{direct} method. The numbers are rounded, the difference is calculated from the full values.

period year	b_{geo} m w.e.	b_{direct} m w.e.	Δb m w.e.
Griesgletscher GG (Funk et al., 1996)			
1961–1979	−1.7	−1.1	−0.6
1979–1986	−2.1	−0.3	−1.8
1986–1991	−5.1	−1.0	−4.1
total	−8.9	−2.4	−6.5
Gulkana Glacier GU (Cox and March, 2004)			
1974–1993	−6.0	−5.8	−0.2
1974–1999	−11.8	−11.2	−0.6
Lemon Creek LC (Miller and Pelto, 1999)			
1957–1989	−11.2	−12.7	1.5
1957–1995	−13.9	−17.1	3.2
total	−18.4	−22.0	3.6
South Cascade SC (Krimmel, 1999)			
1970–1975	0.8	2.4	−1.6
1975–1977	−0.4	−1.6	1.2
1977–1979	−1.9	−1.4	−0.5
1979–1985	−3.6	−5.7	2.1
1985–1997	−11.4	−12.7	1.3
total	−16.5	−19.0	2.5
Storbreen SB (Andreassen, 1999)			
1940–1951	−6.4	−4.9	−1.5
1951–1968	−4.6	−1.3	−3.3
1968–1984	−5.1	−5.4	0.3
1984–1997	−0.7	2.0	−2.7
total	−16.8	−9.6	−7.2
Storglacieren SG (Zemp et al., 2010)			
1959–1969	−3.1	−4.0	0.9
1969–1980	−2.5	−2.9	0.4
1980–1990	1.0	1.3	−0.3
1990–1999	0.7	0.6	0.1
total	−3.9	−5.0	1.1
Zongo Glacier ZG (Soruco et al., 2009)			
1997–2006	−5.1	−7.5	2.4

TCD

4, 1151–1194, 2010

Direct and geodetic mass balances on a multi-annual time scale

A. Fischer

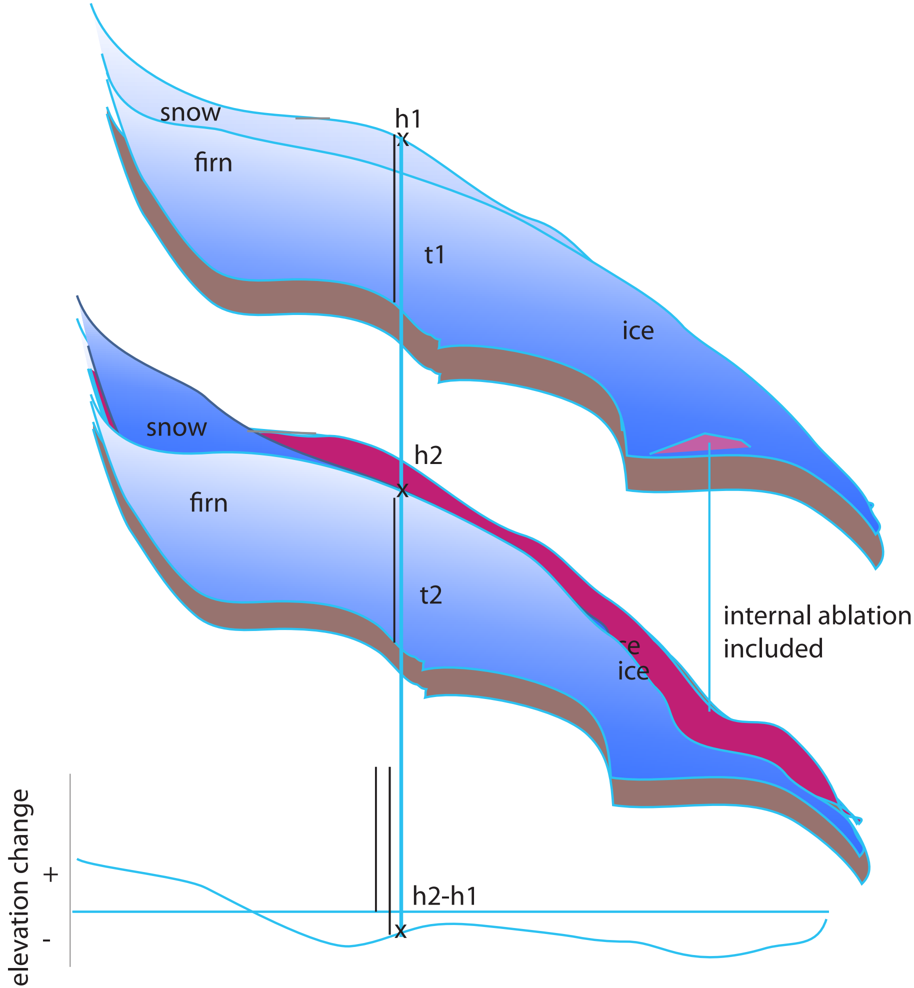

Fig. 1. Calculation of geodetic mass balance between t_1 and t_2.

TCD
4, 1151–1194, 2010

Direct and geodetic mass balances on a multi-annual time scale

A. Fischer

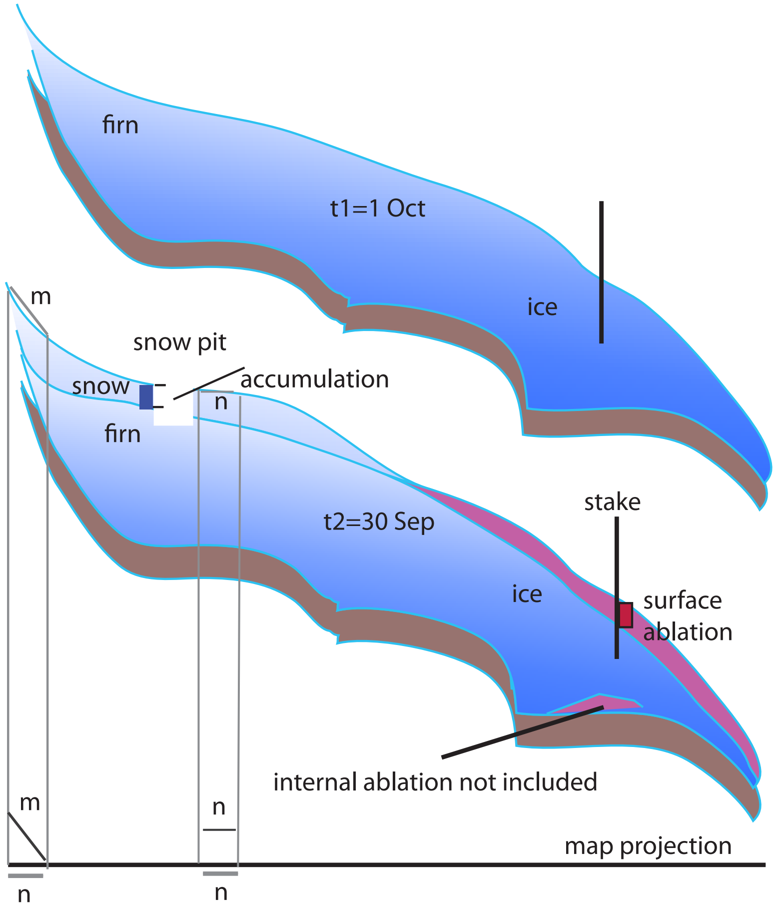

Fig. 2. Determination of mass balance with the direct or glaciological method between 1 October and 30 September.

TCD
4, 1151–1194, 2010

Title Page
Abstract | Introduction
Conclusions | References
Tables | Figures
◀I | ▶I
◀ | ▶
Back | Close
Full Screen / Esc
Printer-friendly Version
Interactive Discussion

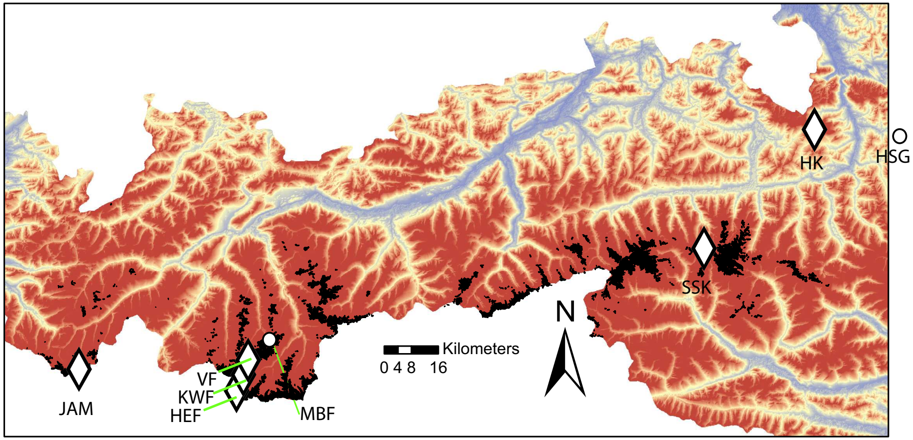

Fig. 3. Location of the Austrian test glaciers JAM,HEF, KWF, VF, SSK and HK (rhombs) and Mittelbergferner/MBF and Hallstätter Glacier/HSG (dots). DEM data from Jarvis et al.

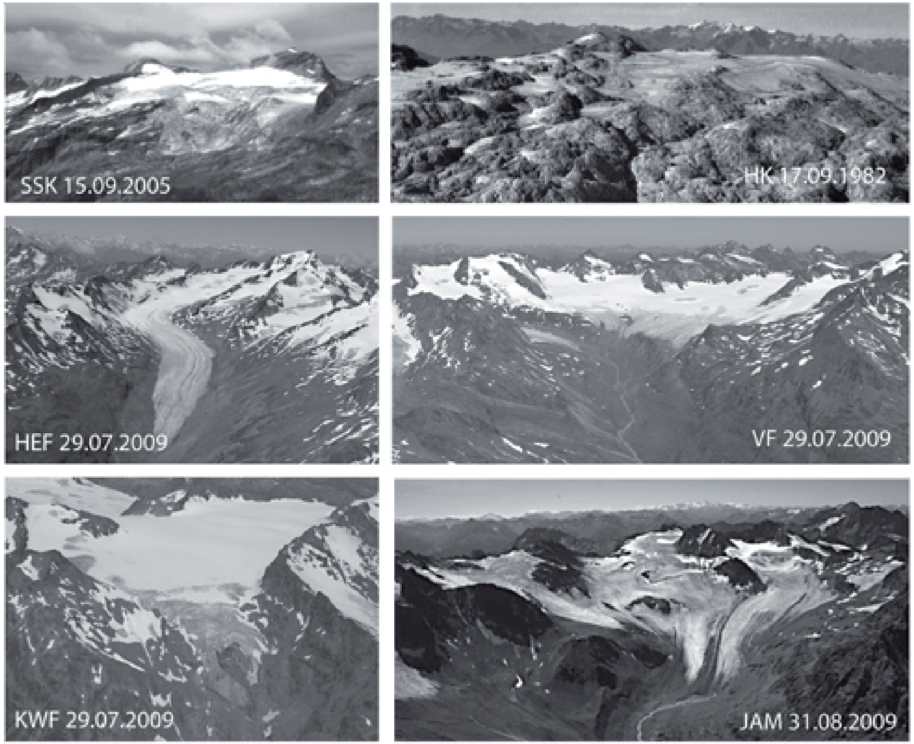

Fig. 4. Oblique photographs of the plateau glaciers SSK and HK, and the valley glaciers HEF, VF, KWF and JAM.

TCD
4, 1151–1194, 2010

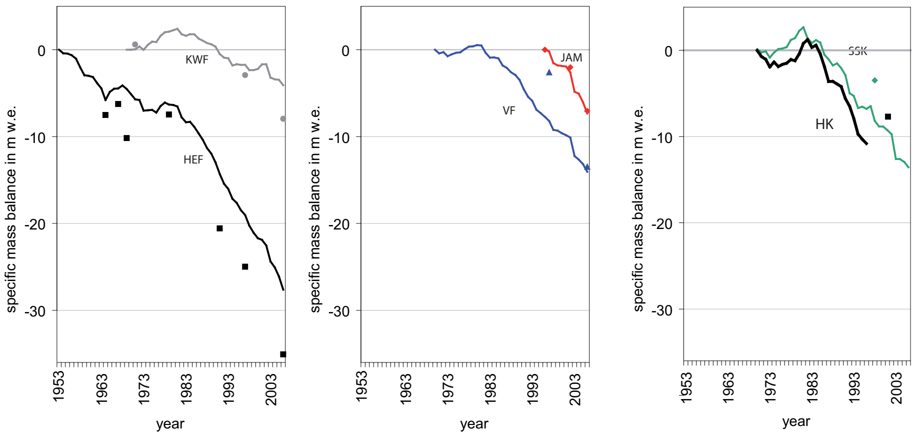

Fig. 5. Cumulative specific mass balance of HEF, KWF, VF, SSK, HK and JAM derived with the direct (lines) and the geodetic (dots) method.

TCD
4, 1151–1194, 2010

Direct and geodetic mass balances on a multi-annual time scale

A. Fischer

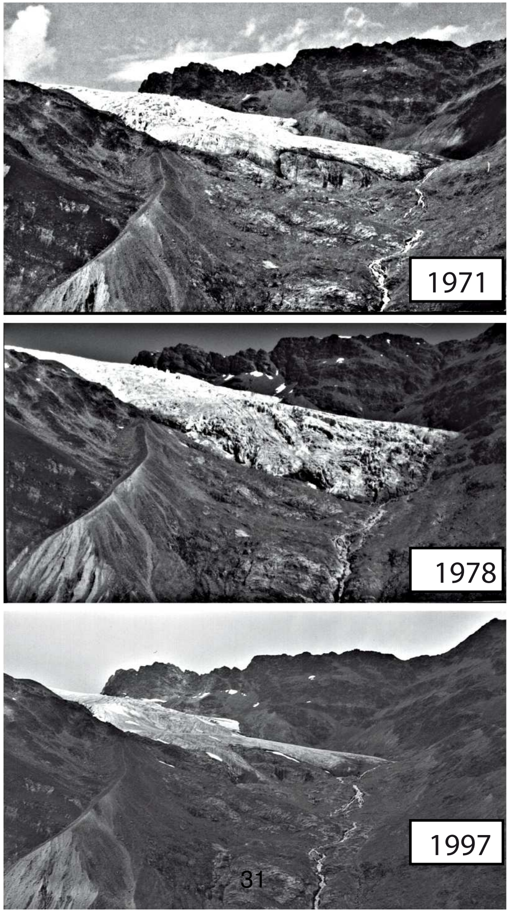

Fig. 6. KWF in 1971, 1978 and 1997.

TCD
4, 1151–1194, 2010

Direct and geodetic mass balances on a multi-annual time scale

A. Fischer

Title Page
Abstract | Introduction
Conclusions | References
Tables | Figures
◀◀ | ▶▶
◀ | ▶
Back | Close
Full Screen / Esc
Printer-friendly Version
Interactive Discussion

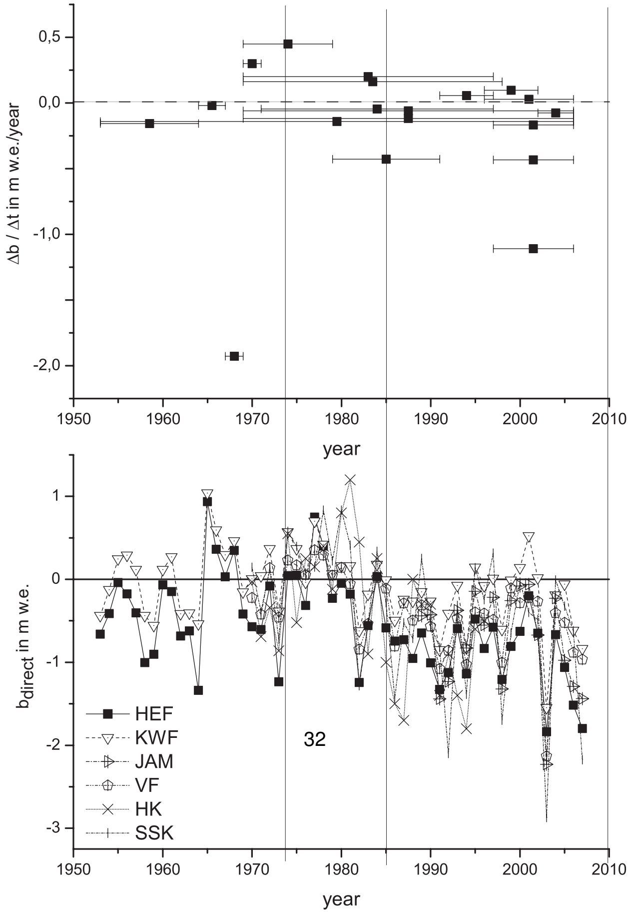

Fig. 7. Comparison of the difference between the geodetic and the direct mass balance per year $\Delta b/\Delta t$ and the direct specific mass balances b_{direct}. The length of the period of the geodetic mass balance mean is indicated with bars.

TCD

4, 1151–1194, 2010

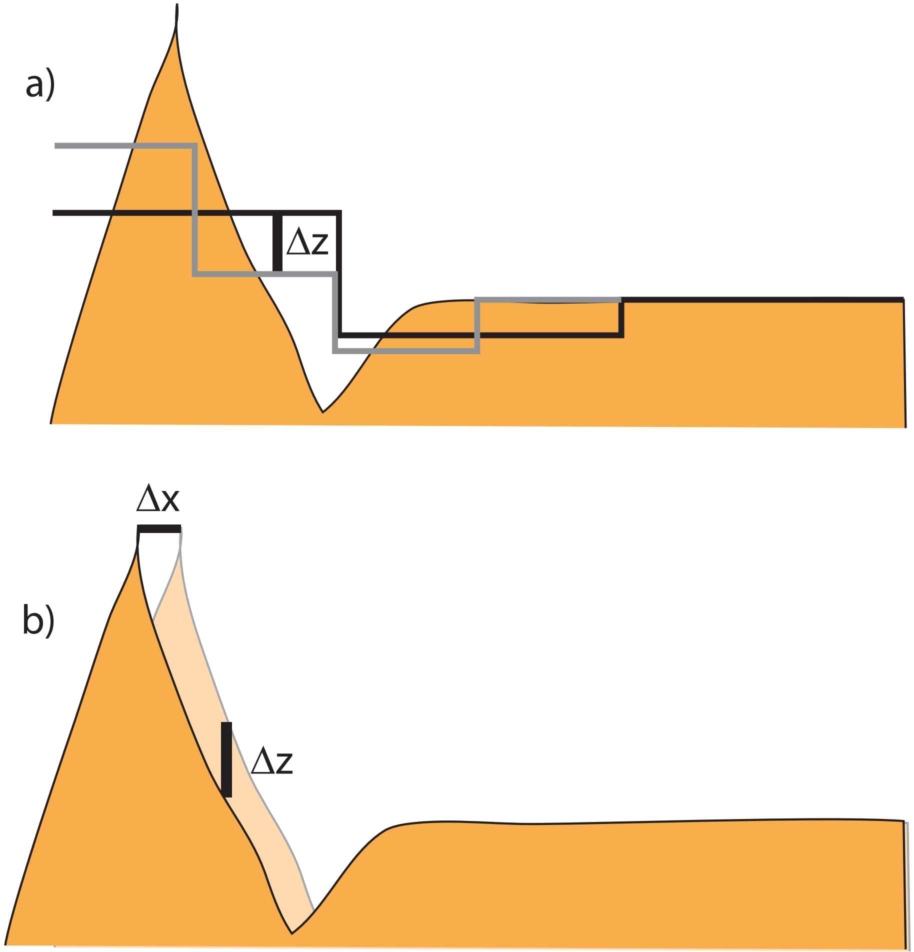

Fig. 8. Vertical errors Δz in a DEM resulting from **(a)** different pixel sizes (grey and black) or **(b)** horizontal errors Δx.

TCD
4, 1151–1194, 2010

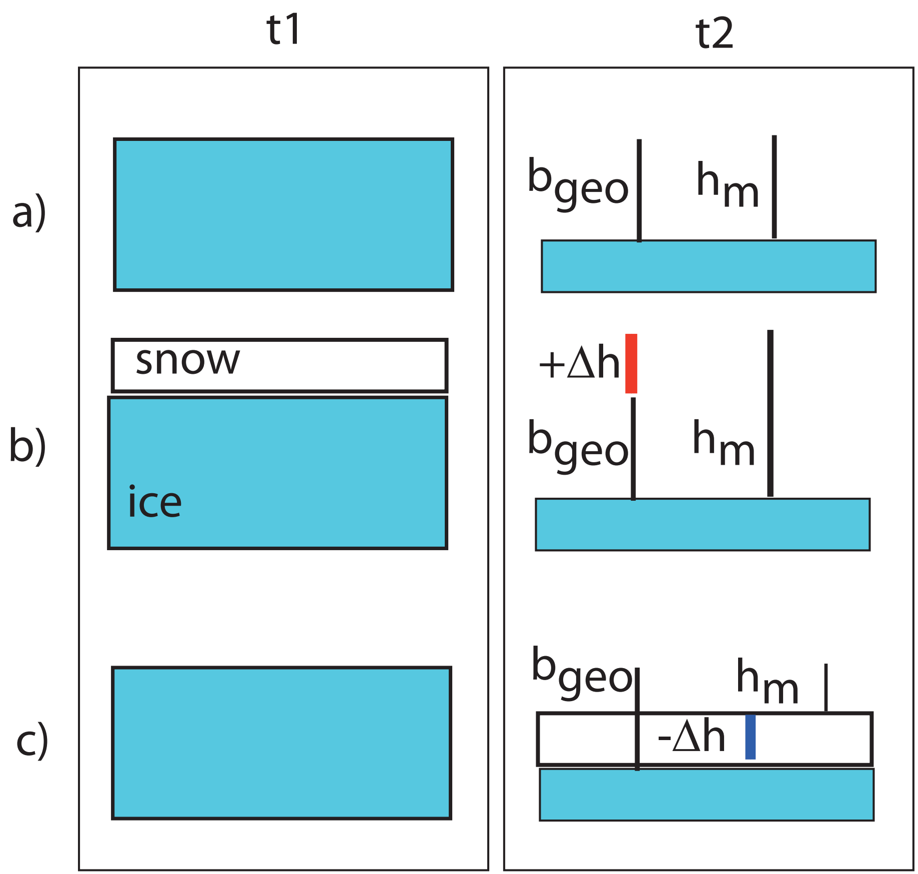

Fig. 9. The effect of a misinterpretation of seasonal snow cover on the measured volume change. The measured elevation change h_m corresponds to the geodetic mass balance b_{geo} in case of no seasonal snow cover **(a)**. If snow covers the glaciers on the DEM at t_1, b_{geo} is overestimated by Δh **(b)**. If snow cover occurs at t_2, b_{geo} is underestimated by Δh.

TCD
4, 1151–1194, 2010

Direct and geodetic mass balances on a multi-annual time scale

A. Fischer

Fig. 10. KWF during the advance at the maximum stage (1985) and after slowing down (2008).

TCD
4, 1151–1194, 2010

Direct and geodetic mass balances on a multi-annual time scale

A. Fischer

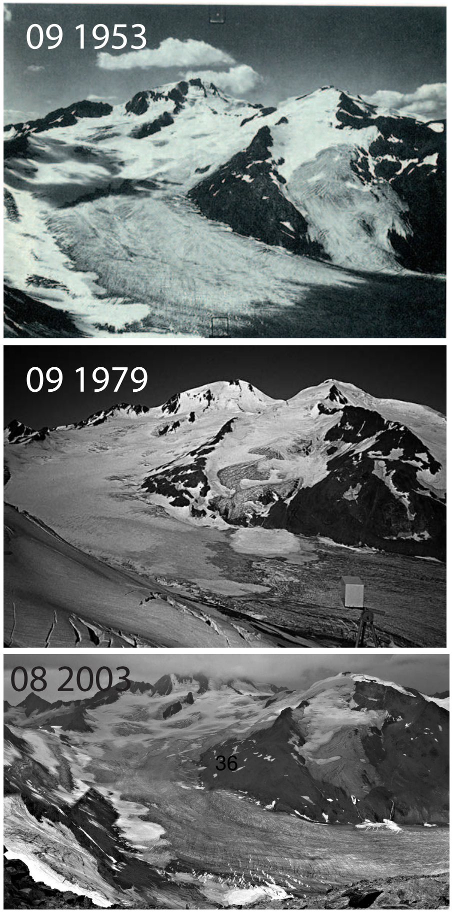

Fig. 11. Firn area of HEF in 1953, 1979 and 2003.

TCD
4, 1151–1194, 2010

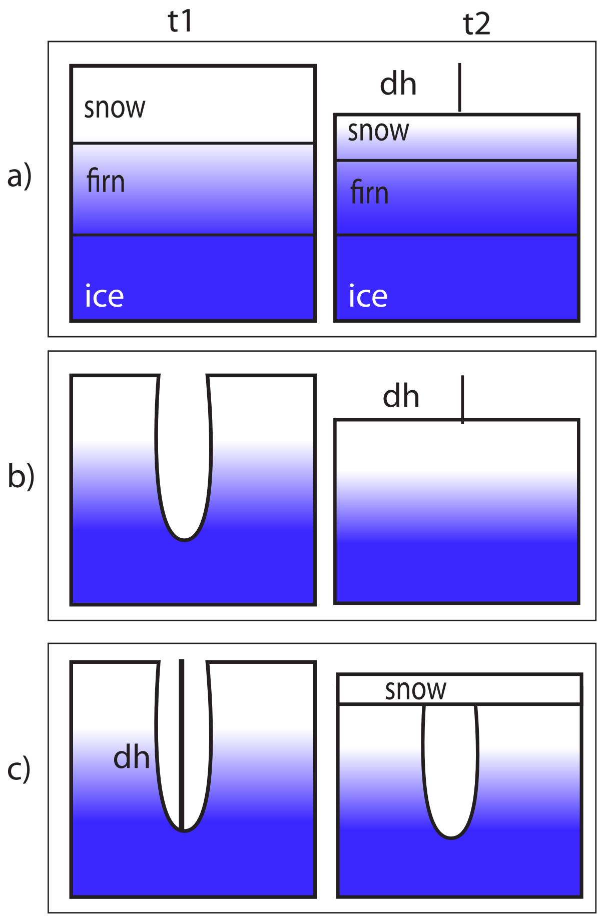

Fig. 12. Thickness changes changes due to changes of density and not due to mass changes: **(a)** densification of the snow and firn, **(b)** closing of a crevasse caused by reduction of flow velocity **(c)** covering of a crevasse by snow.

TCD

4, 1151–1194, 2010

Direct and geodetic mass balances on a multi-annual time scale

A. Fischer

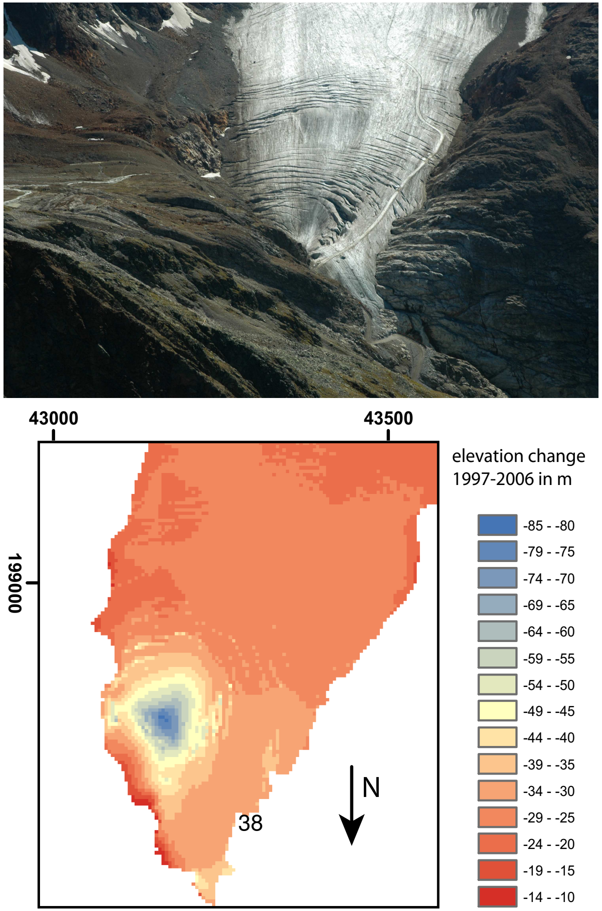

Fig. 13. Radial crevasses and subsidence zone at the tongue of Mittelbergferner in 2006 and the surface elevation change in m between 1997 and 2006.

TCD
4, 1151–1194, 2010

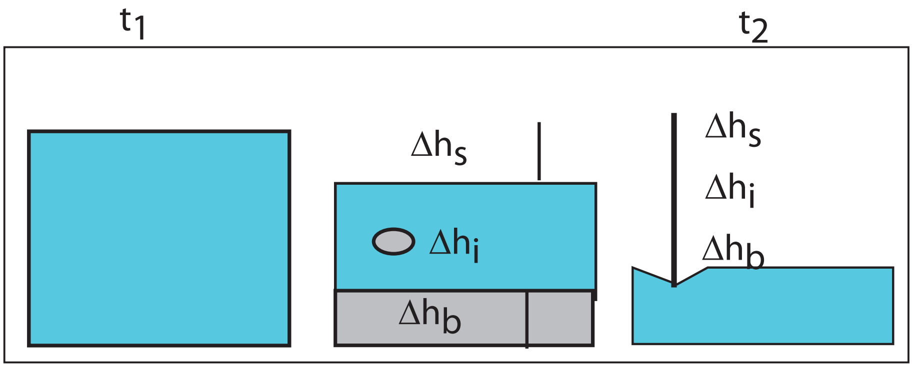

Fig. 14. The total thickness change of a glacier is caused by mass balance at the surface Δh_s and internal and basal mass balance Δh_i and Δh_b if the effects propagate to the surface.

TCD
4, 1151–1194, 2010

TCD
4, 1151–1194, 2010

Direct and geodetic mass balances on a multi-annual time scale

A. Fischer

Title Page
Abstract | Introduction
Conclusions | References
Tables | Figures
◀| |▶
◀ ▶
Back | Close
Full Screen / Esc
Printer-friendly Version
Interactive Discussion

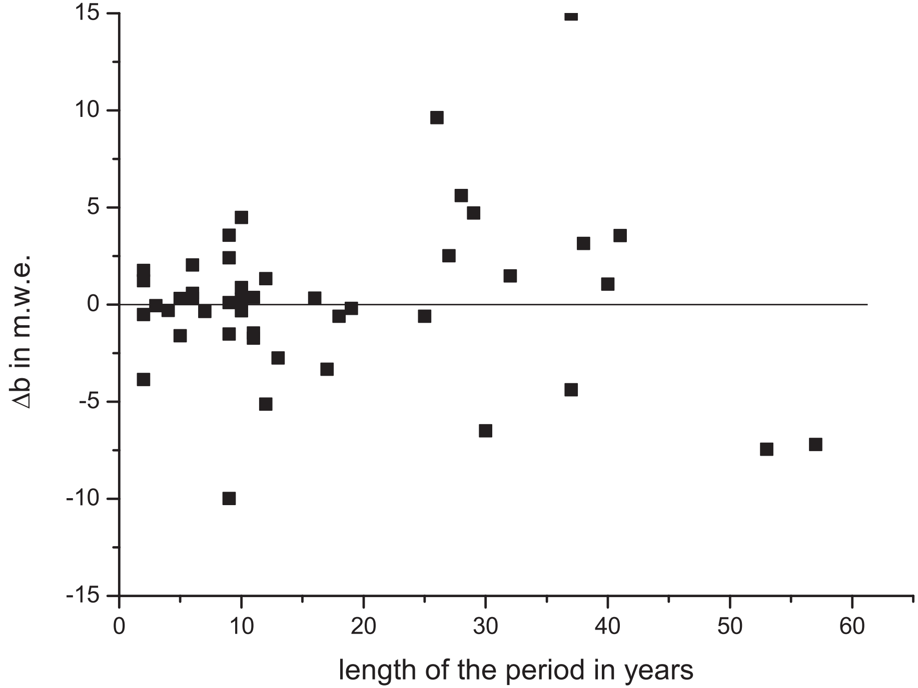

Fig. 15. Length of the period for which the geodetic mass balance b_{geo} is calculated vs. the difference Δb between the geodetic and the direct mass balance.

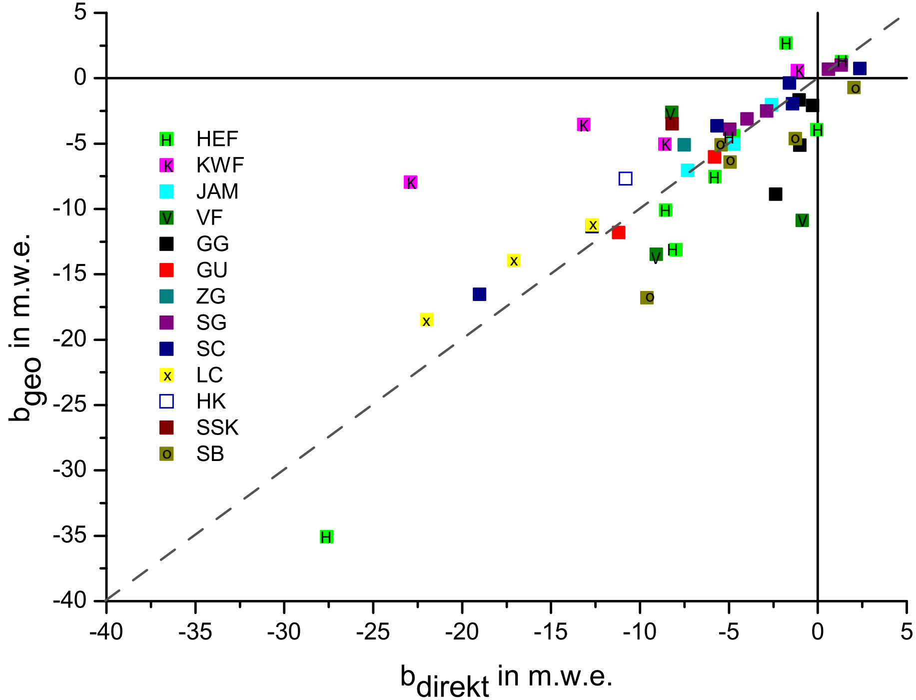

Fig. 16. Comparison of the geodetic b_{geo} and direct b_{direct} mass balance for all 12 glaciers. Griesgletscher … GG, Gulkana Glacier … GU, Zongo Glacier … ZG, Storglacieren … SG, South Cascade … SC, Lemon Creek … LC.

TCD
4, 1151–1194, 2010